The scalar bispectrum during inflation and preheating in single field inflationary models

L. Sriramkumar

Department of Physics, Indian Institute of Technology Madras, Chennai

Raman Research Institute, Bengaluru

April 15, 2013

Proliferation of inflationary models[1]

5-dimensional assisted inflation
anisotropic brane inflation
anomaly-induced inflation
assisted inflation
assisted chaotic inflation
boundary inflation
brane inflation
brane-assisted inflation
brane gas inflation
brane-antibrane inflation
braneworld inflation
Brans-Dicke chaotic inflation
Brans-Dicke inflation
bulky brane inflation
chaotic hybrid inflation
chaotic inflation
chaotic new inflation
D-brane inflation
D-term inflation
dilaton-driven inflation
dilaton-driven brane inflation
double inflation
double D-term inflation
dual inflation
dynamical inflation
dynamical SUSY inflation
eternal inflation
extended inflation
extended open inflation
extended warm inflation
extra dimensional inflation
F-term inflation
F-term hybrid inflation
false vacuum inflation
false vacuum chaotic inflation
fast-roll inflation
first order inflation
gauged inflation
generalised inflation
generalized assisted inflation
generalized slow-roll inflation
gravity driven inflation
Hagedorn inflation
higher-curvature inflation
hybrid inflation
hyperextended inflation
induced gravity inflation
induced gravity open inflation
intermediate inflation
inverted hybrid inflation
isocurvature inflation
K inflation
kinetic inflation
lambda inflation
large field inflation
late D-term inflation
late-time mild inflation
low-scale inflation
low-scale supergravity inflation
M-theory inflation
mass inflation
massive chaotic inflation
moduli inflation
multi-scalar inflation
multiple inflation
multiple-field slow-roll inflation
multiple-stage inflation
natural inflation
natural Chaotic inflation
natural double inflation
natural supergravity inflation
new inflation
next-to-minimal supersymmetric hybrid inflation
non-commutative inflation
non-slow-roll inflation
nonminimal chaotic inflation
old inflation
open hybrid inflation
open inflation
oscillating inflation
polynomial chaotic inflation
polynomial hybrid inflation
power-law inflation
pre-Big-Bang inflation
primary inflation
primordial inflation
quasi-open inflation
quintessential inflation
R-invariant topological inflation
rapid asymmetric inflation
running inflation
scalar-tensor gravity inflation
scalar-tensor stochastic inflation
Seiberg-Witten inflation
single-bubble open inflation
spinodal inflation
stable starobinsky-type inflation
steady-state eternal inflation
steep inflation
stochastic inflation
string-forming open inflation
successful D-term inflation
supergravity inflation
supernatural inflation
superstring inflation
supersymmetric hybrid inflation
supersymmetric inflation
supersymmetric topological inflation
supersymmetric new inflation
synergistic warm inflation
TeV-scale hybrid inflation

A partial list of ever-increasing number of inflationary models!

[1] From E. P. S. Shellard, *The future of cosmology: Observational and computational prospects*, in *The Future of Theoretical Physics and Cosmology*, Eds. G. W. Gibbons, E. P. S. Shellard and S. J. Rankin (Cambridge University Press, Cambridge, England, 2003).

Non-Gaussianities – Pre-Planck status

- If one assumes the bispectrum to be, say, of the so-called *local* form, the WMAP 9-year data constrains the non-Gaussianity parameter $f_{\rm NL}$ to be 37.2 ± 19.9, at 68% confidence level[2].

[2] C. L. Bennett *et al.*, arXiv:1212.5225v1 [astro-ph.CO].

[3] J. Maldacena, JHEP **05**, 013 (2003).

[4] See, for instance, X. Chen, R. Easther and E. A. Lim, JCAP **0706**, 023 (2007).

[5] See, for example, X. Chen, M.-x. Huang, S. Kachru and G. Shiu, JCAP **0701**, 002 (2007).

Non-Gaussianities – Pre-Planck status

- If one assumes the bispectrum to be, say, of the so-called *local* form, the WMAP 9-year data constrains the non-Gaussianity parameter $f_{_{\rm NL}}$ to be 37.2 ± 19.9, at 68% confidence level[2].
- If missions such as Planck indeed detect a large level of non-Gaussianity as suggested by the above mean value of $f_{_{\rm NL}}$, then it can result in a substantial tightening in the constraints on the various inflationary models. For example, canonical scalar field models that lead to nearly scale invariant primordial spectra contain only a small amount of non-Gaussianity and, hence, will cease to be viable[3].

[2] C. L. Bennett *et al.*, arXiv:1212.5225v1 [astro-ph.CO].

[3] J. Maldacena, JHEP **05**, 013 (2003).

[4] See, for instance, X. Chen, R. Easther and E. A. Lim, JCAP **0706**, 023 (2007).

[5] See, for example, X. Chen, M.-x. Huang, S. Kachru and G. Shiu, JCAP **0701**, 002 (2007).

Non-Gaussianities – Pre-Planck status

- If one assumes the bispectrum to be, say, of the so-called *local* form, the WMAP 9-year data constrains the non-Gaussianity parameter $f_{_{\rm NL}}$ to be 37.2 ± 19.9, at 68% confidence level[2].
- If missions such as Planck indeed detect a large level of non-Gaussianity as suggested by the above mean value of $f_{_{\rm NL}}$, then it can result in a substantial tightening in the constraints on the various inflationary models. For example, canonical scalar field models that lead to nearly scale invariant primordial spectra contain only a small amount of non-Gaussianity and, hence, will cease to be viable[3].
- However, it is known that primordial spectra with features can lead to reasonably large non-Gaussianities[4]. Therefore, if the non-Gaussianity parameter $f_{_{\rm NL}}$ actually proves to be large, then either one has to reconcile with the fact that the primordial spectrum contains features or we have to turn our attention to non-canonical scalar field models such as, say, D brane inflation models[5].

[2] C. L. Bennett *et al.*, arXiv:1212.5225v1 [astro-ph.CO].

[3] J. Maldacena, JHEP **05**, 013 (2003).

[4] See, for instance, X. Chen, R. Easther and E. A. Lim, JCAP **0706**, 023 (2007).

[5] See, for example, X. Chen, M.-x. Huang, S. Kachru and G. Shiu, JCAP **0701**, 002 (2007).

Constraints on non-Gaussianities from Planck[6]

- The constraints from Planck on the local form of the non-Gaussianity parameter $f_{_{\rm NL}}$ proves to be 2.7 ± 5.8.

[6] P. A. Ade *et al.*, arXiv:1303.5084 [astro-ph.CO].

Constraints on non-Gaussianities from Planck[6]

- The constraints from Planck on the local form of the non-Gaussianity parameter $f_{\rm NL}$ proves to be 2.7 ± 5.8.
- In other words, preliminary investigations seem to suggest that inflationary models that lead to rather large non-Gaussianities are likely to be ruled out by the data.

[6] P. A. Ade *et al.*, arXiv:1303.5084 [astro-ph.CO].

Plan of the talk

1. Some essential remarks on the evaluation of the scalar power spectrum
2. The scalar bispectrum and the non-Gaussianity parameter – Definitions
3. The Maldacena formalism for evaluating the bispectrum
4. BINGO: An efficient code to numerically compute the bispectrum
5. Constraints from Planck on non-Gaussianities
6. Discriminating power of the non-Gaussianity parameter
7. Contributions to the scalar bispectrum during preheating
8. Summary

This talk is based on

- J. Martin and L. Sriramkumar, *The scalar bispectrum in the Starobinsky model: The equilateral case*, JCAP **1201**, 008 (2012).
- D. K. Hazra, L. Sriramkumar and J. Martin, *BINGO: A code for the efficient computation of the scalar bispectrum*, arXiv:1201.0926v2 [astro-ph.CO].
- D. K. Hazra, J. Martin and L. Sriramkumar, *Scalar bispectrum during preheating in single field inflationary models*, Phys. Rev. D **86**, 063523 (2012).

A few words on the conventions and notations

- We shall work in units such that $c = \hbar = 1$, and define the Planck mass to be $\mathrm{M}_{_{\mathrm{Pl}}}^{2} = (8\,\pi\,G)^{-1}$.

A few words on the conventions and notations

- We shall work in units such that $c = \hbar = 1$, and define the Planck mass to be $\mathrm{M}_{_{\mathrm{Pl}}}^2 = (8\,\pi\,G)^{-1}$.
- As is often done in the context of inflation, we shall assume the background to be described by the spatially flat, Friedmann line-element.

A few words on the conventions and notations

- We shall work in units such that $c = \hbar = 1$, and define the Planck mass to be $\mathrm{M}_{_{\mathrm{Pl}}}^{2} = (8\,\pi\,G)^{-1}$.
- As is often done in the context of inflation, we shall assume the background to be described by the spatially flat, Friedmann line-element.
- We shall denote differentiation with respect to the cosmic and the conformal times t and η by an overdot and an overprime, respectively.

A few words on the conventions and notations

- We shall work in units such that $c = \hbar = 1$, and define the Planck mass to be $\mathrm{M}_{_{\mathrm{Pl}}}^{2} = (8\,\pi\, G)^{-1}$.
- As is often done in the context of inflation, we shall assume the background to be described by the spatially flat, Friedmann line-element.
- We shall denote differentiation with respect to the cosmic and the conformal times t and η by an overdot and an overprime, respectively.
- Further, N shall denote the number of e-folds.

The curvature perturbation and the governing equation

On quantization, the operator corresponding to the curvature perturbation $\mathcal{R}(\eta, \boldsymbol{x})$ can be expressed as

$$\begin{aligned} \hat{\mathcal{R}}(\eta, \boldsymbol{x}) &= \int \frac{\mathrm{d}^3\boldsymbol{k}}{(2\,\pi)^{3/2}}\, \hat{\mathcal{R}}_{\boldsymbol{k}}(\eta)\, \mathrm{e}^{i\,\boldsymbol{k}\cdot\boldsymbol{x}} \\ &= \int \frac{\mathrm{d}^3\boldsymbol{k}}{(2\,\pi)^{3/2}}\, \left[\hat{a}_{\boldsymbol{k}}\, f_{\boldsymbol{k}}(\eta)\, \mathrm{e}^{i\,\boldsymbol{k}\cdot\boldsymbol{x}} + \hat{a}^{\dagger}_{\boldsymbol{k}}\, f^{*}_{\boldsymbol{k}}(\eta)\, \mathrm{e}^{-i\,\boldsymbol{k}\cdot\boldsymbol{x}}\right], \end{aligned}$$

where $\hat{a}_{\boldsymbol{k}}$ and $\hat{a}^{\dagger}_{\boldsymbol{k}}$ are the usual creation and annihilation operators that satisfy the standard commutation relations.

The modes $f_{\boldsymbol{k}}$ are governed by the differential equation

$$f''_{\boldsymbol{k}} + 2\,\frac{z'}{z}\, f'_{\boldsymbol{k}} + k^2\, f_{\boldsymbol{k}} = 0,$$

where $z = a\,\mathrm{M}_{_{\mathrm{Pl}}}\,\sqrt{2\,\epsilon_1}$, with $\epsilon_1 = -\mathrm{d}\ln H/\mathrm{d}N$ being the first slow roll parameter.

The Bunch-Davies initial conditions

While studying the evolution of the curvature perturbation, it often proves to be more convenient to work in terms of the so-called Mukhanov-Sasaki variable $v_{\boldsymbol{k}}$, which is defined as $v_{\boldsymbol{k}} = z\, f_{\boldsymbol{k}}$. In terms of the variable $v_{\boldsymbol{k}}$, the above equation of motion for $f_{\boldsymbol{k}}$ reduces to the following simple form:

$$v_{\boldsymbol{k}}'' + \left(k^2 - \frac{z''}{z}\right) v_{\boldsymbol{k}} = 0.$$

The initial conditions on the perturbations are imposed when the modes are well inside the Hubble radius during inflation.

Usually, it is the so-called Bunch-Davies initial conditions that are imposed on the modes, which amounts to demanding that the Mukhanov-Sasaki variable $v_{\boldsymbol{k}}$ reduces to following Minkowski-like positive frequency form in the sub-Hubble limit[7]:

$$\lim_{k/(a\, H)\to\infty} v_{\boldsymbol{k}} = \frac{1}{\sqrt{2\, k}}\, \mathrm{e}^{-i\, k\, \eta}.$$

[7] T. Bunch and P. C. W. Davies, Proc. Roy. Soc. Lond. A **360**, 117 (1978).

The behavior of modes during inflation

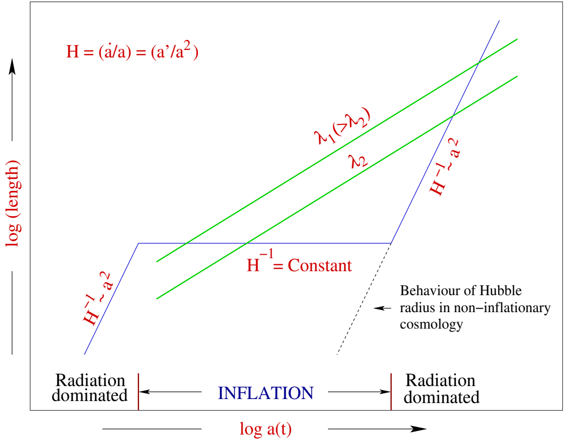

A schematic diagram illustrating the behavior of the physical wavelength $\lambda_{\rm P} \propto a$ (the green lines) and the Hubble radius H^{-1} (the blue line) during inflation and the radiation dominated epochs[8].

[8]See, for example, E. W. Kolb and M. S. Turner, *The Early Universe* (Addison-Wesley Publishing Company, New York, 1990), Fig. 8.4.

The scalar power spectrum

The dimensionless scalar power spectrum $\mathcal{P}_{\rm S}(k)$ is defined in terms of the correlation function of the Fourier modes of the curvature perturbation $\hat{\mathcal{R}}_{\boldsymbol{k}}$ as follows:

$$\langle 0|\hat{\mathcal{R}}_{\boldsymbol{k}}(\eta)\,\hat{\mathcal{R}}_{\boldsymbol{p}}(\eta)|0\rangle = \frac{(2\,\pi)^2}{2\,k^3}\,\mathcal{P}_{\rm S}(k)\;\delta^{(3)}\left(\boldsymbol{k}+\boldsymbol{p}\right),$$

where $|0\rangle$ is the Bunch-Davies vacuum, defined as $\hat{a}_{\boldsymbol{k}}|0\rangle = 0\;\forall\;\boldsymbol{k}$.

In terms of the quantities $f_{\boldsymbol{k}}$ and $v_{\boldsymbol{k}}$, the power spectrum is given by

$$\mathcal{P}_{\rm S}(k) = \frac{k^3}{2\,\pi^2}\,|f_{\boldsymbol{k}}|^2 = \frac{k^3}{2\,\pi^2}\,\left(\frac{|v_{\boldsymbol{k}}|}{z}\right)^2$$

and, analytically, the spectrum is evaluated in the super-Hubble limit, *i.e.* when $k/(a\,H) \to 0$.

As is well known, numerically, the Bunch-Davies initial conditions are imposed on the modes when they are *well inside the Hubble radius*, and the power spectrum is evaluated at suitably late times when the modes are *sufficiently outside*[9].

[9] See, for example, D. S. Salopek, J. R. Bond and J. M. Bardeen, Phys. Rev. D **40**, 1753 (1989); C. Ringeval, Lect. Notes Phys. **738**, 243 (2008).

The scalar bispectrum

The scalar bispectrum $\mathcal{B}_{\rm S}(\boldsymbol{k}_1, \boldsymbol{k}_2, \boldsymbol{k}_3)$ is related to the three point correlation function of the Fourier modes of the curvature perturbation, evaluated towards the end of inflation, say, at the conformal time $\eta_{\rm e}$, as follows[10]:

$$\langle \hat{\mathcal{R}}_{\boldsymbol{k}_1}(\eta_{\rm e})\, \hat{\mathcal{R}}_{\boldsymbol{k}_2}(\eta_{\rm e})\, \hat{\mathcal{R}}_{\boldsymbol{k}_3}(\eta_{\rm e}) \rangle = (2\,\pi)^3\; \mathcal{B}_{\rm S}(\boldsymbol{k}_1, \boldsymbol{k}_2, \boldsymbol{k}_3)\; \delta^{(3)}\,(\boldsymbol{k}_1 + \boldsymbol{k}_2 + \boldsymbol{k}_3)\,.$$

[10] D. Larson *et al.*, Astrophys. J. Suppl. **192**, 16 (2011);
E. Komatsu *et al.*, Astrophys. J. Suppl. **192**, 18 (2011).

The scalar bispectrum

The scalar bispectrum $\mathcal{B}_{\mathrm{S}}(\boldsymbol{k}_1, \boldsymbol{k}_2, \boldsymbol{k}_3)$ is related to the three point correlation function of the Fourier modes of the curvature perturbation, evaluated towards the end of inflation, say, at the conformal time η_{e}, as follows[10]:

$$\langle \hat{\mathcal{R}}_{\boldsymbol{k}_1}(\eta_{\mathrm{e}})\, \hat{\mathcal{R}}_{\boldsymbol{k}_2}(\eta_{\mathrm{e}})\, \hat{\mathcal{R}}_{\boldsymbol{k}_3}(\eta_{\mathrm{e}}) \rangle = (2\,\pi)^3\; \mathcal{B}_{\mathrm{S}}(\boldsymbol{k}_1, \boldsymbol{k}_2, \boldsymbol{k}_3)\; \delta^{(3)}(\boldsymbol{k}_1 + \boldsymbol{k}_2 + \boldsymbol{k}_3)\,.$$

In our discussion below, for the sake of convenience, we shall set

$$\mathcal{B}_{\mathrm{S}}(\boldsymbol{k}_1, \boldsymbol{k}_2, \boldsymbol{k}_3) = (2\,\pi)^{-9/2}\; G(\boldsymbol{k}_1, \boldsymbol{k}_2, \boldsymbol{k}_3).$$

[10] D. Larson *et al.*, Astrophys. J. Suppl. **192**, 16 (2011);
E. Komatsu *et al.*, Astrophys. J. Suppl. **192**, 18 (2011).

The non-Gaussianity parameter $f_{\rm NL}$

The observationally relevant non-Gaussianity parameter $f_{\rm NL}$ is introduced through the relation[11]

$$\mathcal{R}(\eta, \boldsymbol{x}) = \mathcal{R}_{\rm G}(\eta, \boldsymbol{x}) - \frac{3\, f_{\rm NL}}{5}\, \left[\mathcal{R}_{\rm G}^2(\eta, \boldsymbol{x}) - \left\langle \mathcal{R}_{\rm G}^2(\eta, \boldsymbol{x})\right\rangle\right],$$

where $\mathcal{R}_{\rm G}$ denotes the Gaussian quantity, and the factor of $3/5$ arises due to the relation between the Bardeen potential and the curvature perturbation during the matter dominated epoch.

Utilizing the above relation and Wick's theorem, one can arrive at the three point correlation function of the curvature perturbation in Fourier space in terms of the parameter $f_{\rm NL}$. It is found to be

$$\begin{aligned}\langle \hat{\mathcal{R}}_{\boldsymbol{k}_1}\, \hat{\mathcal{R}}_{\boldsymbol{k}_2}\, \hat{\mathcal{R}}_{\boldsymbol{k}_3} \rangle \quad &= \quad -\frac{3\, f_{\rm NL}}{10}\, (2\,\pi)^{5/2}\, \left(\frac{1}{k_1^3\, k_2^3\, k_3^3}\right)\, \delta^{(3)}(\boldsymbol{k}_1 + \boldsymbol{k}_2 + \boldsymbol{k}_3) \\ &\quad \times \left[k_1^3\, \mathcal{P}_{\rm S}(k_2)\, \mathcal{P}_{\rm S}(k_3) + \text{two permutations}\right].\end{aligned}$$

[11] E. Komatsu and D. N. Spergel, Phys. Rev. D **63**, 063002 (2001).

The relation between $f_{\rm NL}$ and the bispectrum

Upon making use of the above expression for the three point function of the curvature perturbation and the definition of the bispectrum, we can, in turn, arrive at the following relation[12]:

$$
\begin{aligned}
f_{\rm NL}(\boldsymbol{k}_1, \boldsymbol{k}_2, \boldsymbol{k}_3) &= -\frac{10}{3}\, (2\,\pi)^{1/2}\, \left(k_1^3\, k_2^3\, k_3^3\right)\, \mathcal{B}_{\rm S}(\boldsymbol{k}_1, \boldsymbol{k}_2, \boldsymbol{k}_3) \\
&\quad \times \left[k_1^3\, \mathcal{P}_{\rm S}(k_2)\, \mathcal{P}_{\rm S}(k_3) + \text{two permutations}\right]^{-1} \\
&= -\frac{10}{3}\, \frac{1}{(2\,\pi)^4}\, \left(k_1^3\, k_2^3\, k_3^3\right)\, G(\boldsymbol{k}_1, \boldsymbol{k}_2, \boldsymbol{k}_3) \\
&\quad \times \left[k_1^3\, \mathcal{P}_{\rm S}(k_2)\, \mathcal{P}_{\rm S}(k_3) + \text{two permutations}\right]^{-1}.
\end{aligned}
$$

[12] See, for instance, S. Hannestad, T. Haugbolle, P. R. Jarnhus and M. S. Sloth, JCAP **1006**, 001 (2010).

The relation between $f_{_{\rm NL}}$ and the bispectrum

Upon making use of the above expression for the three point function of the curvature perturbation and the definition of the bispectrum, we can, in turn, arrive at the following relation[12]:

$$
\begin{aligned}
f_{_{\rm NL}}(\boldsymbol{k}_1, \boldsymbol{k}_2, \boldsymbol{k}_3) &= -\frac{10}{3}\,(2\,\pi)^{1/2}\,\left(k_1^3\, k_2^3\, k_3^3\right)\,\mathcal{B}_{_{\rm S}}(\boldsymbol{k}_1, \boldsymbol{k}_2, \boldsymbol{k}_3)\\
&\quad\times\,\left[k_1^3\,\mathcal{P}_{_{\rm S}}(k_2)\,\mathcal{P}_{_{\rm S}}(k_3) + \text{two permutations}\right]^{-1}\\
&= -\frac{10}{3}\,\frac{1}{(2\,\pi)^4}\,\left(k_1^3\, k_2^3\, k_3^3\right)\,G(\boldsymbol{k}_1, \boldsymbol{k}_2, \boldsymbol{k}_3)\\
&\quad\times\,\left[k_1^3\,\mathcal{P}_{_{\rm S}}(k_2)\,\mathcal{P}_{_{\rm S}}(k_3) + \text{two permutations}\right]^{-1}.
\end{aligned}
$$

Note that, in the equilateral limit, *i.e.* when $k_1 = k_2 = k_3$, this expression for $f_{_{\rm NL}}$ simplifies to

$$
f_{_{\rm NL}}^{\rm eq}(k) = -\frac{10}{9}\,\frac{1}{(2\,\pi)^4}\,\frac{k^6\,G(k)}{\mathcal{P}_{_{\rm S}}^2(k)}.
$$

[12] See, for instance, S. Hannestad, T. Haugbolle, P. R. Jarnhus and M. S. Sloth, JCAP **1006**, 001 (2010).

The action at the cubic order

It can be shown that, the third order term in the action describing the curvature perturbation is given by[13]

$$\mathcal{S}_3[\mathcal{R}] = \mathrm{M}_{_{\mathrm{Pl}}}^2 \int \mathrm{d}\eta \int \mathrm{d}^3\mathbf{x} \biggl[a^2\, \epsilon_1^2\, \mathcal{R}\, \mathcal{R}'^2 + a^2\, \epsilon_1^2\, \mathcal{R}\, (\partial\mathcal{R})^2 - 2\, a\, \epsilon_1\, \mathcal{R}'\, (\partial^i\mathcal{R})\, (\partial_i\chi) + \frac{a^2}{2}\, \epsilon_1\, \epsilon_2'\, \mathcal{R}^2\, \mathcal{R}' + \frac{\epsilon_1}{2}\, (\partial^i\mathcal{R})\, (\partial_i\chi)\, (\partial^2\chi) + \frac{\epsilon_1}{4}\, (\partial^2\mathcal{R})\, (\partial\chi)^2 + \mathcal{F}\left(\frac{\delta\mathcal{L}_2}{\delta\mathcal{R}}\right)\biggr],$$

where $\mathcal{F}(\delta\mathcal{L}_2/\delta\mathcal{R})$ denotes terms involving the variation of the second order action with respect to $\mathcal{R}$, while χ is related to the curvature perturbation $\mathcal{R}$ through the relation

$$\partial^2\chi = a\, \epsilon_1\, \mathcal{R}'.$$

[13] J. Maldacena, JHEP **0305**, 013 (2003);
D. Seery and J. E. Lidsey, JCAP **0506**, 003 (2005);
X. Chen, M.-x. Huang, S. Kachru and G. Shiu, JCAP **0701**, 002 (2007).

Evaluating the bispectrum

At the leading order in the perturbations, one then finds that the three point correlation in Fourier space is described by the integral[14]

$$\langle\hat{\mathcal{R}}_{\boldsymbol{k}_1}(\eta_{\rm e})\,\hat{\mathcal{R}}_{\boldsymbol{k}_2}(\eta_{\rm e})\,\hat{\mathcal{R}}_{\boldsymbol{k}_3}(\eta_{\rm e})\rangle = -i\int_{\eta_{\rm i}}^{\eta_{\rm e}} {\rm d}\eta\; a(\eta)\;\left\langle\left[\hat{\mathcal{R}}_{\boldsymbol{k}_1}(\eta_{\rm e})\,\hat{\mathcal{R}}_{\boldsymbol{k}_2}(\eta_{\rm e})\,\hat{\mathcal{R}}_{\boldsymbol{k}_3}(\eta_{\rm e}), \hat{H}_{\rm I}(\eta)\right]\right\rangle,$$

where $\hat{H}_{\rm I}$ is the Hamiltonian corresponding to the above third order action, while $\eta_{\rm i}$ denotes a sufficiently early time when the initial conditions are imposed on the modes, and $\eta_{\rm e}$ denotes a very late time, say, close to when inflation ends.

Note that, while the square brackets imply the commutation of the operators, the angular brackets denote the fact that the correlations are evaluated in the initial vacuum state (*viz.* the Bunch-Davies vacuum in the situation of our interest).

[14] See, for example, D. Seery and J. E. Lidsey, JCAP **0506**, 003 (2005); X. Chen, Adv. Astron. **2010**, 638979 (2010).

The resulting bispectrum

The quantity $G(\boldsymbol{k}_1, \boldsymbol{k}_2, \boldsymbol{k}_3)$ evaluated towards the end of inflation at the conformal time $\eta = \eta_{\mathrm{e}}$ can be written as[15]

$$
\begin{aligned}
G(\boldsymbol{k}_1, \boldsymbol{k}_2, \boldsymbol{k}_3) \; & \equiv \sum_{C=1}^{7} G_{_C}(\boldsymbol{k}_1, \boldsymbol{k}_2, \boldsymbol{k}_3) \\
& \equiv \mathrm{M}_{_{\mathrm{Pl}}}^{2} \sum_{C=1}^{6} \Big\{ \left[f_{\boldsymbol{k}_1}(\eta_{\mathrm{e}})\, f_{\boldsymbol{k}_2}(\eta_{\mathrm{e}})\, f_{\boldsymbol{k}_3}(\eta_{\mathrm{e}})\right]\, \mathcal{G}_{_C}(\boldsymbol{k}_1, \boldsymbol{k}_2, \boldsymbol{k}_3) \\
& \qquad + \left[f_{\boldsymbol{k}_1}^{*}(\eta_{\mathrm{e}})\, f_{\boldsymbol{k}_2}^{*}(\eta_{\mathrm{e}})\, f_{\boldsymbol{k}_3}^{*}(\eta_{\mathrm{e}})\right]\, \mathcal{G}_{_C}^{*}(\boldsymbol{k}_1, \boldsymbol{k}_2, \boldsymbol{k}_3) \Big\} + G_7(\boldsymbol{k}_1, \boldsymbol{k}_2, \boldsymbol{k}_3),
\end{aligned}
$$

where the quantities $\mathcal{G}_{_C}(\boldsymbol{k}_1, \boldsymbol{k}_2, \boldsymbol{k}_3)$ with $C = (1, 6)$ correspond to the six terms in the interaction Hamiltonian.

The additional, seventh term $G_7(\boldsymbol{k}_1, \boldsymbol{k}_2, \boldsymbol{k}_3)$ arises due to a field redefinition, and its contribution to $G(\boldsymbol{k}_1, \boldsymbol{k}_2, \boldsymbol{k}_3)$ is given by

$$
G_7(\boldsymbol{k}_1, \boldsymbol{k}_2, \boldsymbol{k}_3) = \frac{\epsilon_2(\eta_{\mathrm{e}})}{2} \left(|f_{\boldsymbol{k}_2}(\eta_{\mathrm{e}})|^2\, |f_{\boldsymbol{k}_3}(\eta_{\mathrm{e}})|^2 + \text{two permutations}\right).
$$

[15] J. Martin and L. Sriramkumar, JCAP **1201**, 008 (2012).

The integrals involved

The quantities $\mathcal{G}_C(\boldsymbol{k}_1, \boldsymbol{k}_2, \boldsymbol{k}_3)$ with $C = (1, 6)$ are described by the integrals

$$\mathcal{G}_1(\boldsymbol{k}_1, \boldsymbol{k}_2, \boldsymbol{k}_3) = 2\, i \int_{\eta_{\rm i}}^{\eta_{\rm e}} {\rm d}\eta\, a^2\, \epsilon_1^2\, \left(f_{\boldsymbol{k}_1}^{\ast}\, f_{\boldsymbol{k}_2}^{\prime\ast}\, f_{\boldsymbol{k}_3}^{\prime\ast} + \text{two permutations}\right),$$

$$\mathcal{G}_2(\boldsymbol{k}_1, \boldsymbol{k}_2, \boldsymbol{k}_3) = -2\, i\, \left(\boldsymbol{k}_1 \cdot \boldsymbol{k}_2 + \text{two permutations}\right) \int_{\eta_{\rm i}}^{\eta_{\rm e}} {\rm d}\eta\, a^2\, \epsilon_1^2\, f_{\boldsymbol{k}_1}^{\ast}\, f_{\boldsymbol{k}_2}^{\ast}\, f_{\boldsymbol{k}_3}^{\ast},$$

$$\mathcal{G}_3(\boldsymbol{k}_1, \boldsymbol{k}_2, \boldsymbol{k}_3) = -2\, i \int_{\eta_{\rm i}}^{\eta_{\rm e}} {\rm d}\eta\, a^2\, \epsilon_1^2\, \left[\left(\frac{\boldsymbol{k}_1 \cdot \boldsymbol{k}_2}{k_2^2}\right) f_{\boldsymbol{k}_1}^{\ast}\, f_{\boldsymbol{k}_2}^{\prime\ast}\, f_{\boldsymbol{k}_3}^{\prime\ast} + \text{five permutations}\right],$$

$$\mathcal{G}_4(\boldsymbol{k}_1, \boldsymbol{k}_2, \boldsymbol{k}_3) = i \int_{\eta_{\rm i}}^{\eta_{\rm e}} {\rm d}\eta\, a^2\, \epsilon_1\, \epsilon_2^{\prime}\, \left(f_{\boldsymbol{k}_1}^{\ast}\, f_{\boldsymbol{k}_2}^{\ast}\, f_{\boldsymbol{k}_3}^{\prime\ast} + \text{two permutations}\right),$$

$$\mathcal{G}_5(\boldsymbol{k}_1, \boldsymbol{k}_2, \boldsymbol{k}_3) = \frac{i}{2} \int_{\eta_{\rm i}}^{\eta_{\rm e}} {\rm d}\eta\, a^2\, \epsilon_1^3\, \left[\left(\frac{\boldsymbol{k}_1 \cdot \boldsymbol{k}_2}{k_2^2}\right) f_{\boldsymbol{k}_1}^{\ast}\, f_{\boldsymbol{k}_2}^{\prime\ast}\, f_{\boldsymbol{k}_3}^{\prime\ast} + \text{five permutations}\right],$$

$$\mathcal{G}_6(\boldsymbol{k}_1, \boldsymbol{k}_2, \boldsymbol{k}_3) = \frac{i}{2} \int_{\eta_{\rm i}}^{\eta_{\rm e}} {\rm d}\eta\, a^2\, \epsilon_1^3\, \left\{\left[\frac{k_1^2\, (\boldsymbol{k}_2 \cdot \boldsymbol{k}_3)}{k_2^2\, k_3^2}\right] f_{\boldsymbol{k}_1}^{\ast}\, f_{\boldsymbol{k}_2}^{\prime\ast}\, f_{\boldsymbol{k}_3}^{\prime\ast} + \text{two permutations}\right\},$$

where ϵ_2 is the second slow roll parameter that is defined with respect to the first as follows: $\epsilon_2 = {\rm d} \ln \epsilon_1 / {\rm d}N$.

Evolution of $f_{\boldsymbol{k}}$ on super-Hubble scales

During inflation, when the modes are on super-Hubble scales, it is well known that the solution to $f_{\boldsymbol{k}}$ can be written as

$$f_{\boldsymbol{k}} \simeq A_{\boldsymbol{k}} + B_{\boldsymbol{k}} \int^{\eta} \frac{\mathrm{d}\tilde{\eta}}{z^2(\tilde{\eta})},$$

where $A_{\boldsymbol{k}}$ and $B_{\boldsymbol{k}}$ are k-dependent constants which are determined by the initial conditions imposed on the modes in the sub-Hubble limit.

Therefore, on super-Hubble scales, the mode $f_{\boldsymbol{k}}$ simplifies to

$$f_{\boldsymbol{k}} \simeq A_{\boldsymbol{k}}.$$

Moreover, the leading non-zero contribution to its derivative is determined by the decaying mode, and is given by

$$f_{\boldsymbol{k}}' \simeq \frac{B_{\boldsymbol{k}}}{z^2} = \frac{\bar{B}_{\boldsymbol{k}}}{a^2\, \epsilon_1},$$

where we have set $\bar{B}_{\boldsymbol{k}} = B_{\boldsymbol{k}}/(2\, \mathrm{M}_{_{\mathrm{Pl}}}^2)$.

Splitting the integrals

To begin with, we shall divide each of the integrals $\mathcal{G}_{C}(\boldsymbol{k}_1, \boldsymbol{k}_2, \boldsymbol{k}_3)$, where $C = (1, 6)$, into two parts as follows[16]:

$$\mathcal{G}_{C}(\boldsymbol{k}_1, \boldsymbol{k}_2, \boldsymbol{k}_3) = \mathcal{G}_{C}^{\mathrm{is}}(\boldsymbol{k}_1, \boldsymbol{k}_2, \boldsymbol{k}_3) + \mathcal{G}_{C}^{\mathrm{se}}(\boldsymbol{k}_1, \boldsymbol{k}_2, \boldsymbol{k}_3).$$

The integrals in the first term $\mathcal{G}_{C}^{\mathrm{is}}(\boldsymbol{k}_1, \boldsymbol{k}_2, \boldsymbol{k}_3)$ run from the earliest time (*i.e.* η_{i}) when the smallest of the three wavenumbers k_1, k_2 and k_3 is sufficiently inside the Hubble radius [typically corresponding to $k/(a\, H) \simeq 100$] to the time (say, η_{s}) when the largest of the three wavenumbers is well outside the Hubble radius [say, when $k/(a\, H) \simeq 10^{-5}$].

Then, evidently, the second term $\mathcal{G}_{C}^{\mathrm{se}}(\boldsymbol{k}_1, \boldsymbol{k}_2, \boldsymbol{k}_3)$ will involve integrals which run from the latter time η_{s} to the end of inflation at η_{e}.

[16] D. K. Hazra, L. Sriramkumar and J. Martin, arXiv:1201.0926v2 [astro-ph.CO].

The various times of interest

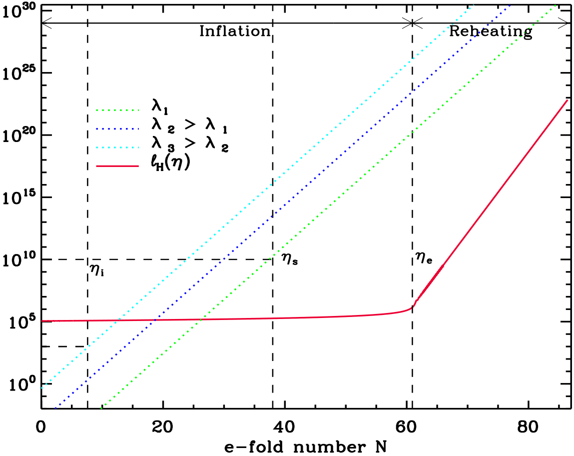

The exact behavior of the physical wavelengths and the Hubble radius plotted as a function of the number of e-folds in the case of the archetypical quadratic potential, which allows us to illustrate the various times of our interest, *viz.* $\eta_{\rm i}$, $\eta_{\rm s}$ and $\eta_{\rm e}$.

Contributions due to the fourth and the seventh terms

Upon using the form of the mode $f_{\boldsymbol{k}}$ and its derivative on super-Hubble scales, the integral appearing in the fourth term can be trivially carried out with the result that the corresponding contribution to the bispectrum can be expressed as

$$G_4^{\rm se}(\boldsymbol{k}_1,\boldsymbol{k}_2,\boldsymbol{k}_3) \simeq i\,{\rm M}_{_{\rm Pl}}^2\,\left[\epsilon_2(\eta_{\rm e})-\epsilon_2(\eta_{\rm s})\right] \times \left[\vert A_{\boldsymbol{k}_1}\vert^2\,\vert A_{\boldsymbol{k}_2}\vert^2\,\left(A_{\boldsymbol{k}_3}\,\bar{B}_{\boldsymbol{k}_3}^{\ast}-A_{\boldsymbol{k}_3}^{\ast}\,\bar{B}_{\boldsymbol{k}_3}\right)+\mbox{two permutations}\right].$$

The Wronskian corresponding to the equation of motion for $f_{\boldsymbol{k}}$ and the standard Bunch-Davies initial conditions can then be utilized to arrive at the following simpler expression:

$$G_4^{\rm se}(\boldsymbol{k}_1,\boldsymbol{k}_2,\boldsymbol{k}_3) \simeq -\frac{1}{2}\,\left[\epsilon_2(\eta_{\rm e})-\epsilon_2(\eta_{\rm s})\right]\,\left[\vert A_{\boldsymbol{k}_1}\vert^2\,\vert A_{\boldsymbol{k}_2}\vert^2+\mbox{two permutations}\right].$$

The first of these terms involving the value of ϵ_2 at $\eta_{\rm e}$ *exactly* cancels the contribution $G_7(\boldsymbol{k}_1,\boldsymbol{k}_2,\boldsymbol{k}_3)$ (with $f_{\boldsymbol{k}}$ set to $A_{\boldsymbol{k}}$).

Note that the remaining term is essentially the same as the one due to the field redefinition, but which is now evaluated on super-Hubble scales (*i.e.* at $\eta_{\rm s}$) rather than at the end of inflation.

The contribution due to the second term

Upon making use of the behavior of the mode $f_{\boldsymbol{k}}$ on super-Hubble scales in the corresponding integral, one obtains the contribution to the bispectrum due to $\mathcal{G}_2^{\rm se}(\boldsymbol{k}_1, \boldsymbol{k}_2, \boldsymbol{k}_3)$ to be

$$G_2^{\rm se}(\boldsymbol{k}_1, \boldsymbol{k}_2, \boldsymbol{k}_3) = -\,2\,i\,{\rm M}_{_{\rm Pl}}^2\;(\boldsymbol{k}_1\cdot\boldsymbol{k}_2 + {\rm two~permutations})\\ \times\,|A_{\boldsymbol{k}_1}|^2\,|A_{\boldsymbol{k}_2}|^2\,|A_{\boldsymbol{k}_3}|^2\;[I_2(\eta_{\rm e},\eta_{\rm s}) - I_2^{\ast}(\eta_{\rm e},\eta_{\rm s})]\,,$$

where the quantity $I_2(\eta_{\rm e},\eta_{\rm s})$ is described by the integral

$$I_2(\eta_{\rm e},\eta_{\rm s}) = \int_{\eta_{\rm s}}^{\eta_{\rm e}} {\rm d}\eta\; a^2\,\epsilon_1^2.$$

Note that, due to the quadratic dependence on the scale factor, actually, $I_2(\eta_{\rm e},\eta_{\rm s})$ is a rapidly growing quantity at late times.

However, the complete super-Hubble contribution to the bispectrum vanishes identically since the integral $I_2(\eta_{\rm e},\eta_{\rm s})$ is a purely real quantity[17].

[17] D. K. Hazra, J. Martin and L. Sriramkumar, Phys. Rev. D **86**, 063523 (2012).

The contributions due to the remaining terms

On super-Hubble scales, one can easily show that the contributions due to the first and the third terms can be written as

$$G_1^{\mathrm{es}}(\boldsymbol{k}_1,\boldsymbol{k}_2,\boldsymbol{k}_3) + G_3^{\mathrm{es}}(\boldsymbol{k}_1,\boldsymbol{k}_2,\boldsymbol{k}_3) = 2\, i\, \mathrm{M}_{\mathrm{Pl}}^2 \Biggl[\left(1 - \frac{\boldsymbol{k}_1\cdot\boldsymbol{k}_2}{k_2^2} - \frac{\boldsymbol{k}_1\cdot\boldsymbol{k}_3}{k_3^2}\right) \vert A_{\boldsymbol{k}_1}\vert^2 \times \left(A_{\boldsymbol{k}_2}\, \bar{B}_{\boldsymbol{k}_2}^{*}\, A_{k_3} \bar{B}_{\boldsymbol{k}_3}^{*} - A_{\boldsymbol{k}_2}^{*} \bar{B}_{\boldsymbol{k}_2}\, A_{\boldsymbol{k}_3}^{*}\, \bar{B}_{\boldsymbol{k}_3}\right) + \text{two permutations}\Biggr]\, I_{13}(\eta_{\mathrm{e}},\eta_{\mathrm{s}}),$$

while the corresponding contributions due to the fifth and the sixth terms are given by

$$G_5^{\mathrm{se}}(\boldsymbol{k}_1,\boldsymbol{k}_2,\boldsymbol{k}_3) + G_6^{\mathrm{se}}(\boldsymbol{k}_1,\boldsymbol{k}_2,\boldsymbol{k}_3) = \frac{i\, \mathrm{M}_{\mathrm{Pl}}^2}{2} \Biggl[\left(\frac{\boldsymbol{k}_1\cdot\boldsymbol{k}_2}{k_2^2} + \frac{\boldsymbol{k}_1\cdot\boldsymbol{k}_3}{k_3^2} + \frac{k_1^2\, (\boldsymbol{k}_2\cdot\boldsymbol{k}_3)}{k_2^2\, k_3^2}\right) \times \vert A_{\boldsymbol{k}_1}\vert^2\, \left(A_{\boldsymbol{k}_2} \bar{B}_{\boldsymbol{k}_2}^{*}\, A_{\boldsymbol{k}_3} \bar{B}_{\boldsymbol{k}_3}^{*} - A_{\boldsymbol{k}_2}^{*} \bar{B}_{\boldsymbol{k}_2}\, A_{\boldsymbol{k}_3}^{*}\, \bar{B}_{\boldsymbol{k}_3}\right) + \text{two permutations}\Biggr]\, I_{56}(\eta_{\mathrm{e}},\eta_{\mathrm{s}}),$$

where the quantities $I_{13}(\eta_{\mathrm{e}},\eta_{\mathrm{s}})$ and $I_{56}(\eta_{\mathrm{e}},\eta_{\mathrm{s}})$ are described by the integrals

$$I_{13}(\eta_{\mathrm{e}},\eta_{\mathrm{s}}) = \int_{\eta_{\mathrm{s}}}^{\eta_{\mathrm{e}}} \frac{\mathrm{d}\eta}{a^2} \quad \text{and} \quad I_{56}(\eta_{\mathrm{e}},\eta_{\mathrm{s}}) = \int_{\eta_{\mathrm{s}}}^{\eta_{\mathrm{e}}} \frac{\mathrm{d}\eta}{a^2}\, \epsilon_1.$$

The complete super-Hubble contribution to $f_{_{\rm NL}}^{\rm eq}$

To arrive at the complete super-Hubble contribution to the non-Gaussianity parameter $f_{_{\rm NL}}$, let us restrict ourselves to the equilateral limit for simplicity.

In such a case, the sum of the super-Hubble contributions due to the first, the third, the fifth and the sixth terms to $f_{_{\rm NL}}^{\rm eq}$ is found to be

$$f_{_{\rm NL}}^{{\rm eq}\,({\rm se})}(k) \simeq -\frac{5\,i\,{\rm M}_{_{\rm Pl}}^2}{18}\,\left(\frac{A_{\boldsymbol{k}}^2\,\bar{B}_{\boldsymbol{k}}^{*\,2}-A_{\boldsymbol{k}}^{*\,2}\,\bar{B}_{\boldsymbol{k}}^2}{\vert A_{\boldsymbol{k}}\vert^2}\right)\,\left[12\,I_{13}(\eta_{\rm e},\eta_{\rm s})-\frac{9}{4}\,I_{56}(\eta_{\rm e},\eta_{\rm s})\right],$$

where we have made use of the fact that $f_{\boldsymbol{k}}\simeq A_{\boldsymbol{k}}$ at late times in order to arrive at the power spectrum.

An estimate of the super-Hubble contribution to $f_{\rm NL}^{\rm eq}$

Consider power law inflation of the form $a(\eta) = a_1\, (\eta/\eta_1)^{\gamma+1}$, where a_1 and η_1 are constants, while γ is a free index. For such an expansion, the first slow roll parameter is a constant, and is given by $\epsilon_1 = (\gamma+2)/(\gamma+1)$.

In such a case, one can easily obtain that

$$f_{\rm NL}^{{\rm eq}\,({\rm se})}(k) = \frac{5}{72\,\pi}\, \left[12 - \frac{9\,(\gamma+2)}{\gamma+1}\right]\, \Gamma^2\left(\gamma+\frac{1}{2}\right)\, 2^{2\,\gamma+1}\, (2\,\gamma+1)\, (\gamma+2)$$
$$\times\, (\gamma+1)^{-2\,(\gamma+1)}\, \sin\,(2\,\pi\,\gamma)\, \left[1 - \frac{H_{\rm s}}{H_{\rm e}}\, {\rm e}^{-3\,(N_{\rm e}-N_{\rm s})}\right]\, \left(\frac{k}{a_{\rm s}\, H_{\rm s}}\right)^{-(2\,\gamma+1)}.$$

and, in arriving at this expression, for convenience, we have set η_1 to be η_s.

For $\gamma = -(2+\varepsilon)$, where $\varepsilon \simeq 10^{-2}$, the above estimate for $f_{_{\rm NL}}$ reduces to

$$f_{\rm NL}^{{\rm eq}\,({\rm se})}(k) \lesssim -\frac{5\,\varepsilon^2}{9}\, \left(\frac{k_{\rm s}}{a_{\rm s}\, H_{\rm s}}\right)^3 \simeq -10^{-19},$$

where, in obtaining the final value, we have set $k_{\rm s}/(a_{\rm s}\, H_{\rm s}) = 10^{-5}$.

Convergence on the upper limit

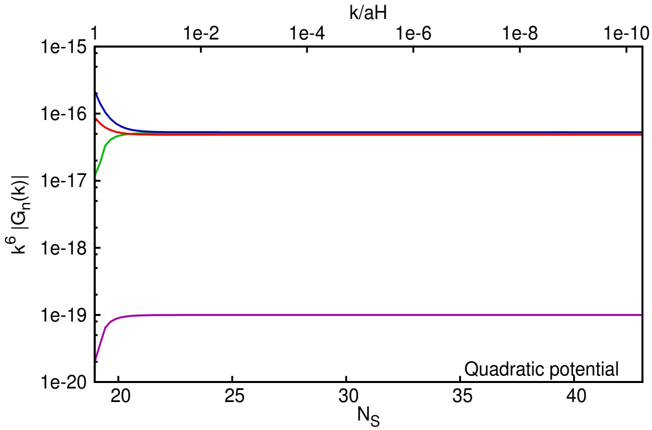

Focusing on the equilateral limit, the quantities k^6 times the absolute values of $G_1 + G_3$ (in green), G_2 (in red), $G_4 + G_7$ (in blue) and $G_5 + G_6$ (in purple), evaluated numerically, have been plotted as a function of the upper limit of the integrals involved for a given mode in the case of the conventional, quadratic inflationary potential. Evidently, the integrals converge rapidly once the mode leaves the Hubble radius.

Implementation of the cut-off in the sub-Hubble limit

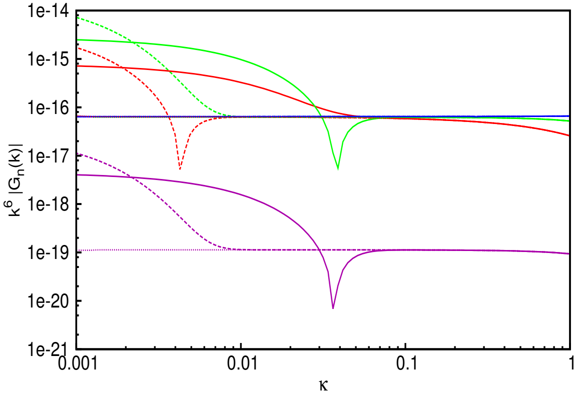

The various contributions to the bispectrum, obtained numerically, have been plotted (with the same choice of colors as in the previous figure) as a function of the cut-off parameter κ for a given mode and a fixed upper limit [corresponding to $k/(a\,H)=10^{-5}$] in the case of the quadratic inflationary potential. The solid, dashed and the dotted lines correspond to integrating from $k/(a\,H)$ of 10^2, 10^3 and 10^4, respectively. Clearly, $\kappa=0.1$ seems to be an optimal value.

The spectral dependence in power law inflation

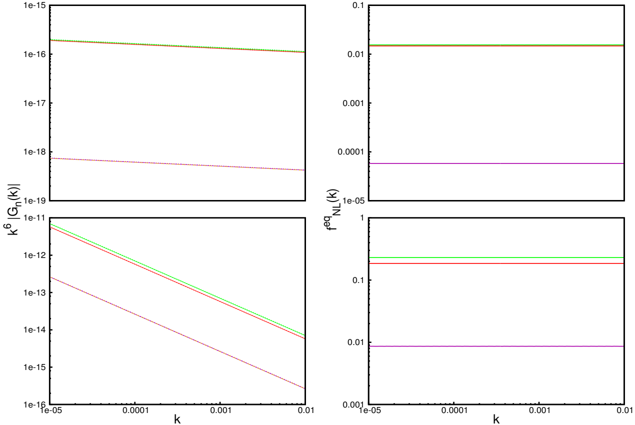

The different non-zero contributions to the bispectrum, viz. the quantities k^6 times the absolute values of $G_1 + G_3$ (in green), G_2 (in red) and $G_5 + G_6$ (in purple), in power law inflation (on the left) and the corresponding contributions to the non-Gaussianity parameter $f_{\rm NL}^{\rm eq}$ (on the right), arrived at using BINGO (BIspectra and Non-Gaussianity Operator), have been plotted as solid lines for two different values of γ (above and below). The dots on the lines represent the analytical results.

The Starobinsky model

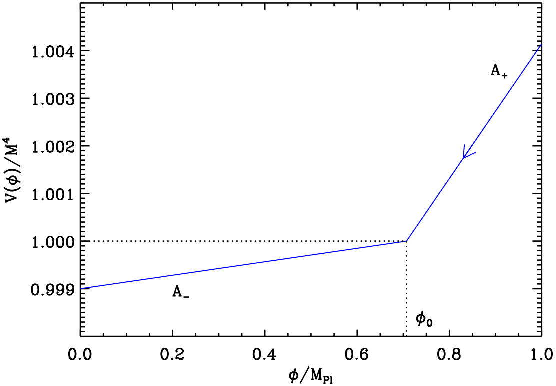

The Starobinsky model involves the canonical scalar field which is described by the potential[18]

$$V(\phi) = \begin{cases} V_0 + A_+ \, (\phi - \phi_0) & \text{for } \phi > \phi_0, \\ V_0 + A_- \, (\phi - \phi_0) & \text{for } \phi < \phi_0. \end{cases}$$

[18] A. A. Starobinsky, Sov. Phys. JETP Lett. **55**, 489 (1992).

Evolution of the slow roll parameters

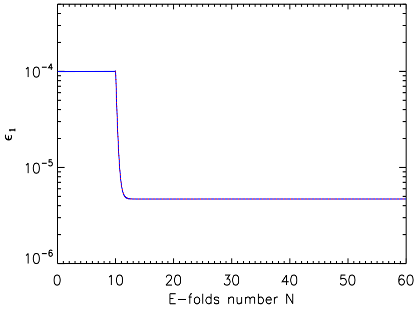

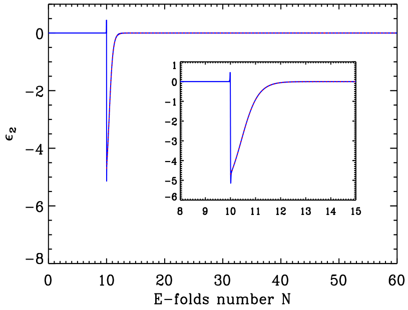

The evolution of the first (on the left) and the second (on the right) slow roll parameters ϵ_1 and ϵ_2 in the Starobinsky model. While the solid blue curves describe the numerical results, the dotted red curves (which lie right below the blue curves and hence not very evident!) represent the corresponding analytical expressions.

The scalar power spectrum in the Starobinsky model

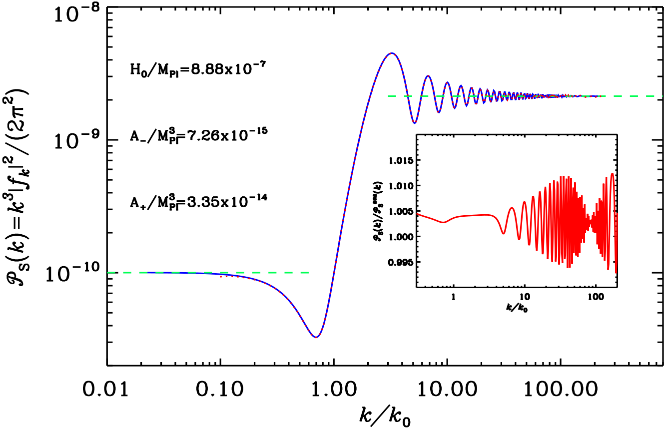

The scalar power spectrum in the Starobinsky model[19]. While the solid blue curve denotes the analytic result, the red dots represent the scalar power spectrum that has been obtained through a complete numerical integration of the background as well as the perturbations.

[19] J. Martin and L. Sriramkumar, JCAP **1201**, 008 (2012).

Comparison in the case of the Starobinsky model

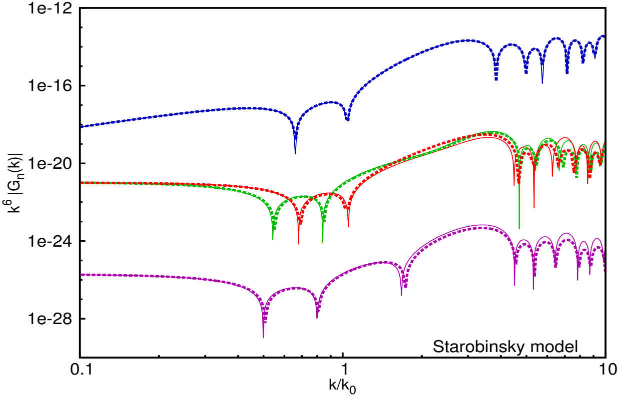

A comparison of the analytical expressions (the solid curves) with the corresponding results from BINGO (the dashed curves) in the case of the Starobinsky model. While the contribution due to the term $G_4 + G_7$ appears in blue, we have chosen the same colors to denote the other contributions to the bispectrum as in the earlier figure[20].

[20] See, J. Martin and L. Sriramkumar, JCAP **1201**, 008 (2012);
In this context, also see, F. Arroja, A. E. Romano and M. Sasaki, Phys. Rev. D **84**, 123503 (2011); F. Arroja and M. Sasaki, JCAP **1208**, 012 (2012).

Comparison for an arbitrary triangular configuration

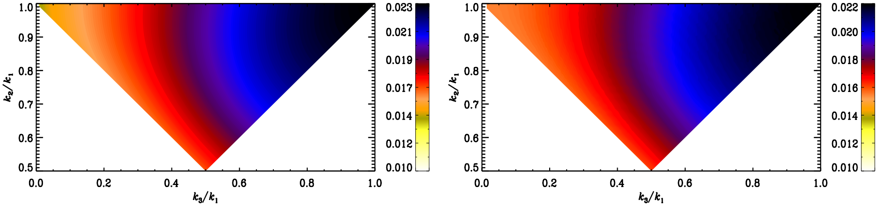

A comparison of the analytical results (on the left) for the non-Gaussianity parameter $f_{\rm NL}$ with the results from BINGO (on the right) for a generic triangular configuration of the wavevectors in the case of the standard quadratic potential. It should be mentioned that the contributions due to the first, the second, the third and the seventh terms (i.e. G_1, G_2, G_3 and G_7) have been taken into account in arriving at these results. The maximum difference between the numerical and the analytic results is found to be about 5%.

Template bispectra

For comparison with the observations, the bispectrum is often expressed as follows[21]:

$$G(\boldsymbol{k}_1, \boldsymbol{k}_2, \boldsymbol{k}_3) = f_{\rm NL}^{\rm loc}\, G_{\rm loc}(\boldsymbol{k}_1, \boldsymbol{k}_2, \boldsymbol{k}_3) + f_{\rm NL}^{\rm eq}\, G_{\rm eq}(\boldsymbol{k}_1, \boldsymbol{k}_2, \boldsymbol{k}_3) + f_{\rm NL}^{\rm orth}\, G_{\rm orth}(\boldsymbol{k}_1, \boldsymbol{k}_2, \boldsymbol{k}_3),$$

where $f_{\rm NL}^{\rm loc}$, $f_{\rm NL}^{\rm eq}$ and $f_{\rm NL}^{\rm orth}$ are free parameters that are to be estimated, and the local, the equilateral, and the orthogonal template bispectra are given by:

$$\begin{aligned}
G_{\rm loc}(\boldsymbol{k}_1, \boldsymbol{k}_2, \boldsymbol{k}_3) &= \frac{6}{5}\left[\frac{(2\,\pi^2)^2}{k_1^3\, k_2^3\, k_3^3}\right] \left(k_1^3\, \mathcal{P}_{\rm S}(k_2)\, \mathcal{P}_{\rm S}(k_3) + \text{two permutations}\right),\\
G_{\rm eq}(\boldsymbol{k}_1, \boldsymbol{k}_2, \boldsymbol{k}_3) &= \frac{3}{5}\left[\frac{(2\,\pi^2)^2}{k_1^3\, k_2^3\, k_3^3}\right) \biggl(6\, k_2\, k_3^2\, \mathcal{P}_{\rm S}(k_1)\, \mathcal{P}_{\rm S}^{2/3}(k_2)\, \mathcal{P}_{\rm S}^{1/3}(k_3) - 3\, k_3^3\, \mathcal{P}_{\rm S}(k_1)\, \mathcal{P}_{\rm S}(k_2)\\
&\quad -2\, k_1\, k_2\, k_3\, \mathcal{P}_{\rm S}^{2/3}(k_1)\, \mathcal{P}_{\rm S}^{2/3}(k_2)\, \mathcal{P}_{\rm S}^{2/3}(k_3) + \text{five permutations}\biggr),\\
G_{\rm orth}(\boldsymbol{k}_1, \boldsymbol{k}_2, \boldsymbol{k}_3) &= \frac{3}{5}\left[\frac{(2\,\pi^2)^2}{k_1^3\, k_2^3\, k_3^3}\right] \biggl(18\, k_2\, k_3^2\, \mathcal{P}_{\rm S}(k_1)\, \mathcal{P}_{\rm S}^{2/3}(k_2)\, \mathcal{P}_{\rm S}^{1/3}(k_3) - 9\, k_3^3\, \mathcal{P}_{\rm S}(k_1)\, \mathcal{P}_{\rm S}(k_2)\\
&\quad -8\, k_1\, k_2\, k_3\, \mathcal{P}_{\rm S}^{2/3}(k_1)\, \mathcal{P}_{\rm S}^{2/3}(k_2)\, \mathcal{P}_{\rm S}^{2/3}(k_3) + \text{five permutations}\biggr).
\end{aligned}$$

The basis $(f_{\rm NL}^{\rm loc}, f_{\rm NL}^{\rm eq}, f_{\rm NL}^{\rm orth})$ for the three-point function is considered to be large enough to encompass a range of interesting models.

[21] C. L. Bennett *et al.*, arXiv:1212.5225v1 [astro-ph.CO].

Illustration of the template bispectra

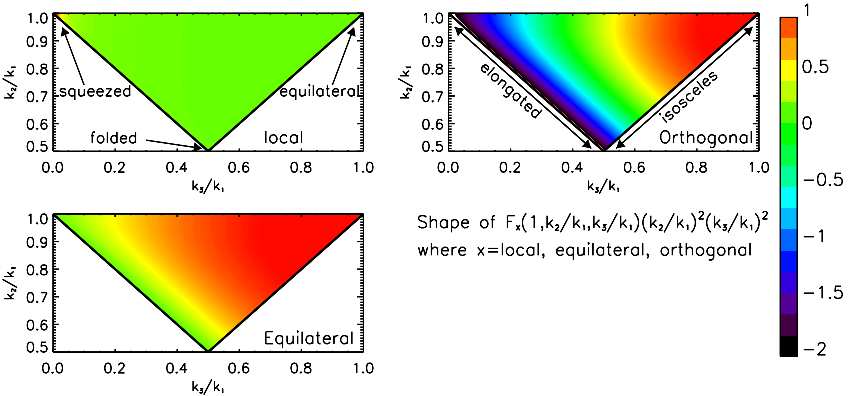

An illustration of the three template basis bispectra, viz. the local (top left), the equilateral (bottom) and the orthogonal (top right) forms for a generic triangular configuration of the wavevectors[22].

[22] E. Komatsu, Class. Quantum Grav. **27**, 124010 (2010).

Constraints on $f_{\rm NL}$

The constraints on the non-Gaussianity parameters from the recent Planck data are as follows[23]:

$$\begin{aligned} f_{\rm NL}^{\rm loc} &= 2.7 \pm 5.8, \\ f_{\rm NL}^{\rm eq} &= -42 \pm 75, \\ f_{\rm NL}^{\rm orth} &= -25 \pm 39. \end{aligned}$$

It should be stressed here that these are constraints on the primordial values.

Also, the constraints on each of the $f_{\rm NL}$ parameters have been arrived at assuming that the other two parameters are zero.

[23] P. A. R. Ade *et al.*, arXiv:1303.5084 [astro-ph.CO].

Post-inflationary dynamics and non-linearities

- Post-inflationary dynamics, such as the curvaton and the modulated reheating scenarios can also lead to non-Gaussianities[24]. The strong constraints on $f_{\rm NL}^{\rm loc}$ from Planck suggests that the primordial non-Gaussianities are unlikely to have been generated post-inflation.
- Also, non-linear evolution, leading to and immediately after the epoch of decoupling, have been to shown to result in non-Gaussianities at the level of $\mathcal{O}(f_{\rm NL}) \sim 1 - 5$[25].

Clearly, these contributions need to be understood satisfactorily before the observational limits can be used to arrive at constraints on inflationary models.

---

[24] See, for instance, D. Langlois and T. Takahashi, arXiv:1301.3319v1 [astro-ph.CO].

[25] C. Pitrou, J.-P. Uzan and F. Bernardeau, JCAP **1007**, 003 (2010);
S.-C. Su, E. A. Lim and E. P. S. Shellard, arXiv:1212.6968v1 [astro-ph.CO].

Punctuated inflation

Punctuated inflation is a scenario wherein a brief period of rapid roll inflation or even a departure from inflation is sandwiched between two epochs of slow roll inflation[26].

[26] R. K. Jain, P. Chingangbam, J.-O. Gong, L. Sriramkumar and T. Souradeep, JCAP **0901**, 009 (2009); R. K. Jain, P. Chingangbam, L. Sriramkumar and T. Souradeep, Phys. Rev. D **82**, 023509 (2010).

[27] R. Allahverdi, K. Enqvist, J. Garcia-Bellido, A. Jokinen and A. Mazumdar, JCAP **0706**, 019 (2007).

Punctuated inflation

Punctuated inflation is a scenario wherein a brief period of rapid roll inflation or even a departure from inflation is sandwiched between two epochs of slow roll inflation[26].

Such a scenario can be achieved in inflaton potentials such as[27]

$$V(\phi) = \left(m^2/2\right)\,\phi^2 - \left(\sqrt{2\,\lambda\,(n-1)}\,m/n\right)\,\phi^n + (\lambda/4)\,\phi^{2(n-1)},$$

where $n > 2$ is an integer. This potential contains a point of inflection located at

$$\phi_0 = \left[\frac{2\,m^2}{(n-1)\,\lambda}\right]^{\frac{1}{2\,(n-2)}},$$

and it is the presence of this inflection point that admits punctuated inflation.

[26] R. K. Jain, P. Chingangbam, J.-O. Gong, L. Sriramkumar and T. Souradeep, JCAP **0901**, 009 (2009); R. K. Jain, P. Chingangbam, L. Sriramkumar and T. Souradeep, Phys. Rev. D **82**, 023509 (2010).

[27] R. Allahverdi, K. Enqvist, J. Garcia-Bellido, A. Jokinen and A. Mazumdar, JCAP **0706**, 019 (2007).

Punctuated inflation

Punctuated inflation is a scenario wherein a brief period of rapid roll inflation or even a departure from inflation is sandwiched between two epochs of slow roll inflation[26].

Such a scenario can be achieved in inflaton potentials such as[27]

$$V(\phi) = \left(m^2/2\right)\,\phi^2 - \left(\sqrt{2\,\lambda\,(n-1)}\,m/n\right)\,\phi^n + (\lambda/4)\,\phi^{2\,(n-1)},$$

where $n > 2$ is an integer. This potential contains a point of inflection located at

$$\phi_0 = \left[\frac{2\,m^2}{(n-1)\,\lambda}\right]^{\frac{1}{2\,(n-2)}},$$

and it is the presence of this inflection point that admits punctuated inflation.

These scenarios can lead to a sharp drop in power on large scales and result in an improved fit to the data at the low multipoles.

---

[26] R. K. Jain, P. Chingangbam, J.-O. Gong, L. Sriramkumar and T. Souradeep, JCAP **0901**, 009 (2009); R. K. Jain, P. Chingangbam, L. Sriramkumar and T. Souradeep, Phys. Rev. D **82**, 023509 (2010).

[27] R. Allahverdi, K. Enqvist, J. Garcia-Bellido, A. Jokinen and A. Mazumdar, JCAP **0706**, 019 (2007).

Inflaton potentials with a step

Given a potential $V(\phi)$, one can introduce the step in the following fashion[28]:

$$V_{\rm step}(\phi) = V(\phi)\, \left[1 + \alpha\, \tanh\left(\frac{\phi - \phi_0}{\Delta\phi}\right)\right],$$

where, evidently, α, ϕ_0 and $\Delta\phi$ denote the height, the location, and the width of the step, respectively.

[28] J. A. Adams, B. Cresswell and R. Easther, Phys. Rev. D **64**, 123514 (2001).

[29] L. Covi, J. Hamann, A. Melchiorri, A. Slosar and I. Sorbera, Phys. Rev. D **74**, 083509 (2006); M. J. Mortonson, C. Dvorkin, H. V. Peiris and W. Hu, Phys. Rev. D **79**, 103519 (2009); D. K. Hazra, M. Aich, R. K. Jain, L. Sriramkumar and T. Souradeep, JCAP **1010**, 008 (2010).

Inflaton potentials with a step

Given a potential $V(\phi)$, one can introduce the step in the following fashion[28]:

$$V_{\rm step}(\phi) = V(\phi)\,\left[1+\alpha\,\tanh\left(\frac{\phi-\phi_0}{\Delta\phi}\right)\right],$$

where, evidently, α, ϕ_0 and $\Delta\phi$ denote the height, the location, and the width of the step, respectively.

Such a step in potentials $V(\phi)$ which otherwise only result in slow roll lead to oscillatory features in the scalar power spectrum that provide a better fit to the outliers near $\ell = 20$ and $\ell = 44$[29].

[28] J. A. Adams, B. Cresswell and R. Easther, Phys. Rev. D **64**, 123514 (2001).

[29] L. Covi, J. Hamann, A. Melchiorri, A. Slosar and I. Sorbera, Phys. Rev. D **74**, 083509 (2006); M. J. Mortonson, C. Dvorkin, H. V. Peiris and W. Hu, Phys. Rev. D **79**, 103519 (2009); D. K. Hazra, M. Aich, R. K. Jain, L. Sriramkumar and T. Souradeep, JCAP **1010**, 008 (2010).

Oscillating inflation potentials

Potentials containing oscillatory terms are encountered in string theory. A popular example is the axion monodromy model, which is described by the potential[30]

$$V(\phi) = \lambda \left[\phi + \alpha \cos\left(\frac{\phi}{\beta} + \delta\right)\right].$$

30 R. Flauger, L. McAllister, E. Pajer, A. Westphal and G. Xu, JCAP **1006**, 009 (2010).

31 M. Aich, D. K. Hazra, L. Sriramkumar and T. Souradeep, arXiv:1106.2798v2 [astro-ph.CO].

32 C. Pahud, M. Kamionkowski and A. R. Liddle, Phys. Rev. D **79**, 083503 (2009).

Oscillating inflation potentials

Potentials containing oscillatory terms are encountered in string theory. A popular example is the axion monodromy model, which is described by the potential[30]

$$V(\phi) = \lambda \left[\phi + \alpha \cos\left(\frac{\phi}{\beta} + \delta\right)\right].$$

Interestingly, such a potential leads to non-local features – *i.e.* a certain characteristic and repeated pattern that extends over a wide range of scales – in the primordial spectrum which result in an improved fit to the data[31].

30 R. Flauger, L. McAllister, E. Pajer, A. Westphal and G. Xu, JCAP **1006**, 009 (2010).

31 M. Aich, D. K. Hazra, L. Sriramkumar and T. Souradeep, arXiv:1106.2798v2 [astro-ph.CO].

32 C. Pahud, M. Kamionkowski and A. R. Liddle, Phys. Rev. D **79**, 083503 (2009).

Oscillating inflation potentials

Potentials containing oscillatory terms are encountered in string theory. A popular example is the axion monodromy model, which is described by the potential[30]

$$V(\phi) = \lambda \left[\phi + \alpha \cos\left(\frac{\phi}{\beta} + \delta\right)\right].$$

Interestingly, such a potential leads to non-local features – *i.e.* a certain characteristic and repeated pattern that extends over a wide range of scales – in the primordial spectrum which result in an improved fit to the data[31].

Another potential that has been considered in this context is the conventional quadratic potential which is superposed by sinusoidal oscillations as follows[32]:

$$V(\phi) = \frac{1}{2}\, m^2\, \phi^2 \left[1 + \alpha \sin\left(\frac{\phi}{\beta} + \delta\right)\right].$$

[30] R. Flauger, L. McAllister, E. Pajer, A. Westphal and G. Xu, JCAP **1006**, 009 (2010).

[31] M. Aich, D. K. Hazra, L. Sriramkumar and T. Souradeep, arXiv:1106.2798v2 [astro-ph.CO].

[32] C. Pahud, M. Kamionkowski and A. R. Liddle, Phys. Rev. D **79**, 083503 (2009).

The various models of interest

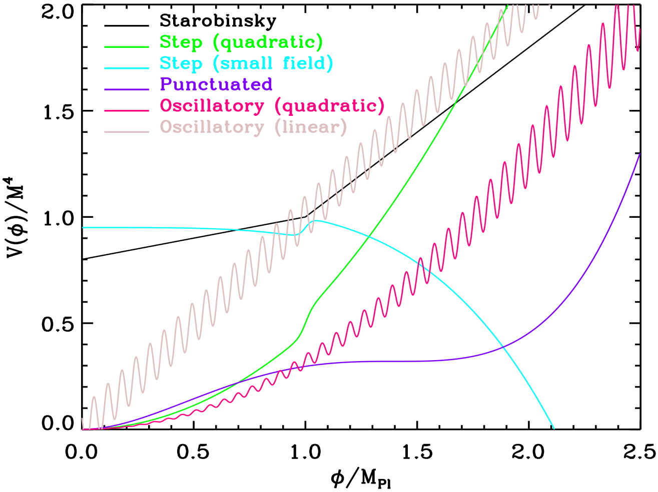

Illustration of the potentials in the different inflationary models of our interest.

Inflationary models leading to features

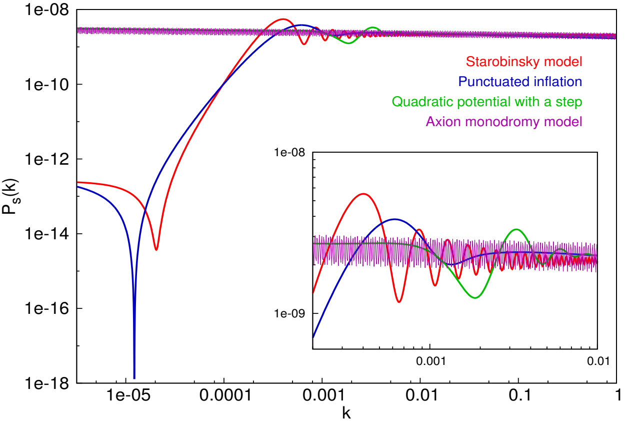

The scalar power spectra in the different inflationary models that lead to a better fit to the CMB data than the conventional power law spectrum[33].

[33] R. K. Jain, P. Chingangbam, J.-O. Gong, L. Sriramkumar and T. Souradeep, JCAP **0901**, 009 (2009);
D. K. Hazra, M. Aich, R. K. Jain, L. Sriramkumar and T. Souradeep, JCAP **1010**, 008 (2010);
M. Aich, D. K. Hazra, L. Sriramkumar and T. Souradeep, arXiv:1106.2798v2 [astro-ph.CO].

$f_{\rm NL}^{\rm eq}$ in punctuated inflation

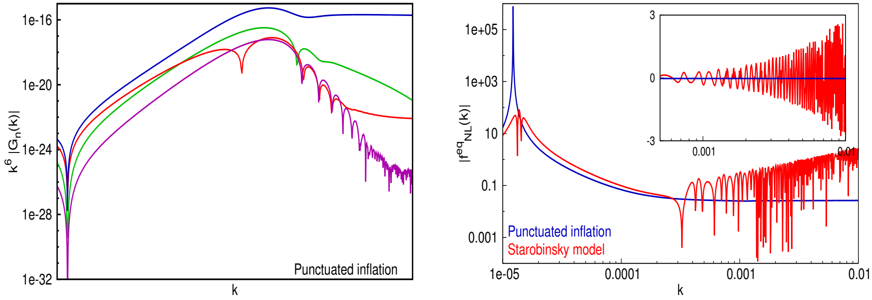

The contributions to the bispectrum due to the various terms (on the left), and the absolute value of $f_{\rm NL}^{\rm eq}$ due to the dominant contribution (on the right), in the punctuated inflationary scenario[34]. The absolute value of $f_{\rm NL}^{\rm eq}$ in a Starobinsky model that closely resembles the power spectrum in punctuated inflation has also been displayed. The large difference in $f_{\rm NL}^{\rm eq}$ between punctuated inflation and the Starobinsky model can be attributed to the considerable difference in the background dynamics.

[34] D. K. Hazra, L. Sriramkumar and J. Martin, arXiv:1201.0926v1 [astro-ph.CO].

$f_{\rm NL}^{\rm eq}$ in models with a step

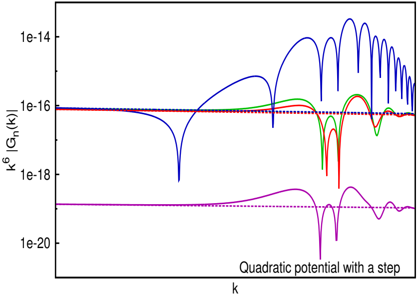

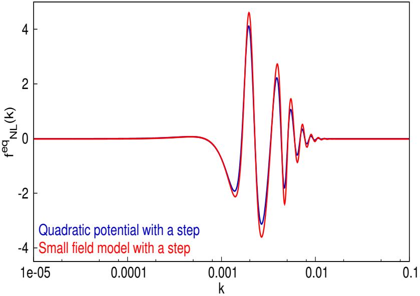

The contributions due to the various terms (on the left) and $f_{\rm NL}^{\rm eq}$ due to the dominant contribution (on the right) when a step has been introduced in the popular chaotic inflationary model involving the quadratic potential[35]. The $f_{\rm NL}^{\rm eq}$ that arises in a small field model with a step has also been illustrated[36]. The background dynamics in these two models are very similar, and hence they lead to almost the same $f_{\rm NL}^{\rm eq}$.

[35] X. Chen, R. Easther and E. A. Lim, JCAP **0706**, 023 (2007); JCAP **0804**, 010 (2008);
P. Adshead, W. Hu, C. Dvorkin and H. V. Peiris, Phys. Rev. D **84**, 043519 (2011);
P. Adshead, C. Dvorkin, W. Hu and E. A. Lim, Phys. Rev. D **85**, 023531 (2012).

[36] D. K. Hazra, L. Sriramkumar and J. Martin, arXiv:1201.0926v2 [astro-ph.CO].

$f_{\rm NL}^{\rm eq}$ in the axion monodromy model

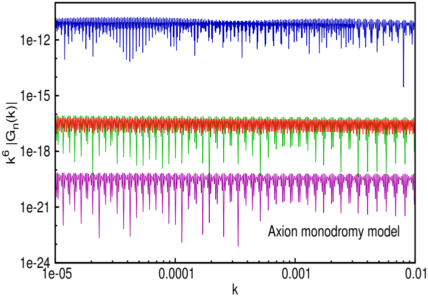

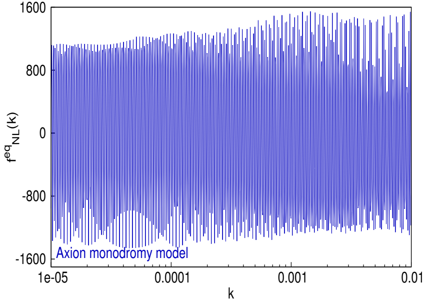

The contributions due to the various terms (on the left) and $f_{\rm NL}^{\rm eq}$ due to the dominant contribution (on the right) in the axion monodromy model[37]. The modulations in the potential give rise to a certain resonant behavior, leading to a large $f_{\rm NL}^{\rm eq}$[38].

[37] D. K. Hazra, L. Sriramkumar and J. Martin, arXiv:1201.0926v1 [astro-ph.CO].

[38] S. Hannestad, T. Haugbolle, P. R. Jarnhus and M. S. Sloth, JCAP **1006**, 001 (2010); R. Flauger and E. Pajer, JCAP **1101**, 017 (2011).

$f_{\rm NL}^{\rm eq}$ in the axion monodromy model

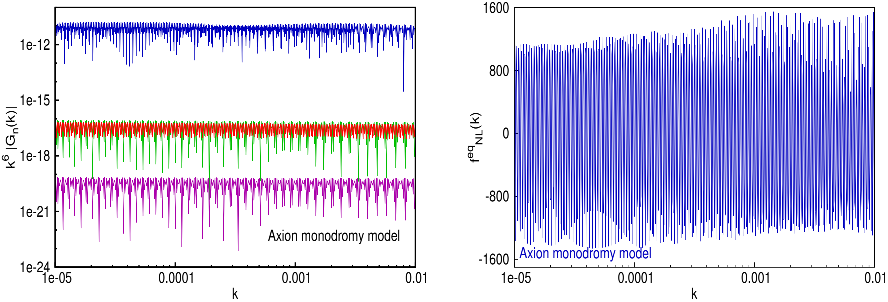

The contributions due to the various terms (on the left) and $f_{\rm NL}^{\rm eq}$ due to the dominant contribution (on the right) in the axion monodromy model[37]. The modulations in the potential give rise to a certain resonant behavior, leading to a large $f_{\rm NL}^{\rm eq}$[38].

In contrast, the quadratic potential with superposed oscillations does not lead to such a large level of non-Gaussianity.

[37] D. K. Hazra, L. Sriramkumar and J. Martin, arXiv:1201.0926v1 [astro-ph.CO].

[38] S. Hannestad, T. Haugbolle, P. R. Jarnhus and M. S. Sloth, JCAP **1006**, 001 (2010);
R. Flauger and E. Pajer, JCAP **1101**, 017 (2011).

Behavior of the field in a quadratic potential

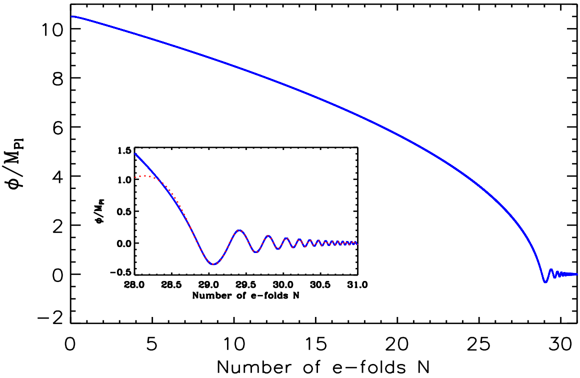

The behavior of the scalar field during the epochs of inflation and preheating have been plotted as a function of the number of e-folds for the case of the conventional chaotic inflationary model described by the quadratic potential. The blue curve denotes the numerical result, while the dotted red curve in the inset represents the analytical result.

Evolution of the slow roll parameters

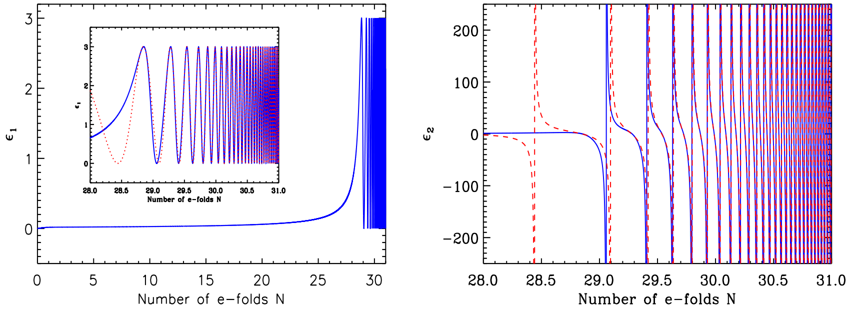

The evolution of the first (on the left) and the second (on the right) slow roll parameters ϵ_1 and ϵ_2 as the field is oscillating about the quadratic minimum. As in the previous figure, the blue curves represent the numerical result, while the dashed red curves denote the analytical result during preheating. Note that, for the choice parameters and initial conditions that we have worked with, ϵ_1 turns unity at the e-fold of $N_{\rm e} \simeq 28.3$, indicating the termination of inflation at the point.

The curvature perturbation during preheating

Though the modes of cosmological interest are well outside the Hubble radius at late times, the conventional super-Hubble solutions to the modes $f_{\boldsymbol{k}}$ during inflation do not *a priori* hold at the time of preheating.

This is due to the fact that, though $k/(a\,H)$ is small, because of the oscillating scalar field, the quantity z''/z itself can vanish during preheating. In fact, when the values of the parameters fall in certain domains known as the resonant bands, the modes display an instability[39].

However, for the case of quadratic minima associated with mass, say, m, it can be shown that, the conventional, inflationary, super-Hubble solutions indeed apply provided the following two conditions are satisfied:

$$\left(\frac{k}{a\,H}\right)^2 \frac{H^2}{m^2} \ll 1 \quad \text{and} \quad \left(\frac{k}{a\,H}\right)^2 \frac{H}{3\,m} \ll 1.$$

Given that, $H < m$ immediately after inflation, it is evident that the first of the above two conditions will be satisfied if the second is[40].

[39] F. Finelli and R. Brandenberger, Phys. Rev. Lett. **82**, 1362 (1999).

[40] K. Jedamzik, M. Lemoine and J. Martin, JCAP **1009**, 034 (2010); JCAP **1004** 021 (2010).

Analytic solution during preheating

Up to the order k^2, the dominant, super-Hubble, inflationary solution to the mode $f_{\boldsymbol{k}}$ is given by

$$f_{\boldsymbol{k}}(\eta) \simeq A_{\boldsymbol{k}} \left[1 - k^2 \int^{\eta} \frac{\mathrm{d}\bar{\eta}}{z^2(\bar{\eta})} \int^{\bar{\eta}} \mathrm{d}\tilde{\eta}\, z^2(\tilde{\eta})\right].$$

The solutions for the background available when the potential around the minimum behaves quadratically allows us to actually evaluate the above integrals in a closed form.

We find that, during this epoch, the growing mode of the curvature perturbation can be written as

$$f_{\boldsymbol{k}} = A_{\boldsymbol{k}} \left[1 - \frac{1}{5} \left(\frac{k}{a\,H}\right)^2 \frac{H}{m} \tan\left(m\,t + \Delta\right)\right],$$

where Δ is a constant of integration[41].

[41] R. Easther, R. Flauger and J. B. Gilmore, JCAP **1104**, 027 (2011).

Comparison with the numerical result

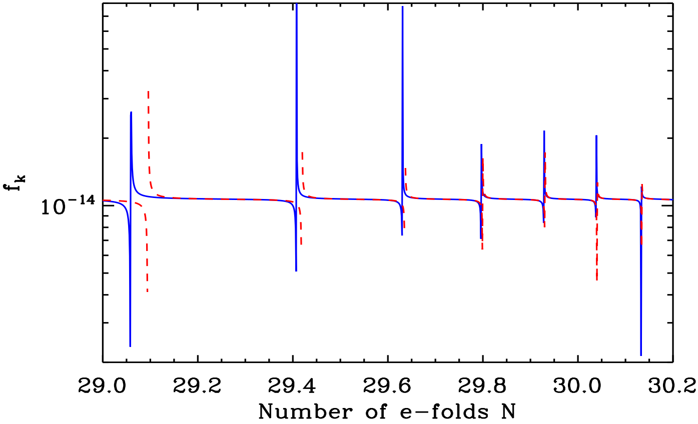

The behavior of the curvature perturbation during preheating. The blue curve denotes the numerical result, while the dashed red curve represents the super-Hubble analytical solution. We have chosen to work with a very small scale mode that leaves the Hubble radius at about two e-folds before the end of inflation.

An illustration of the accuracy of the analytical result

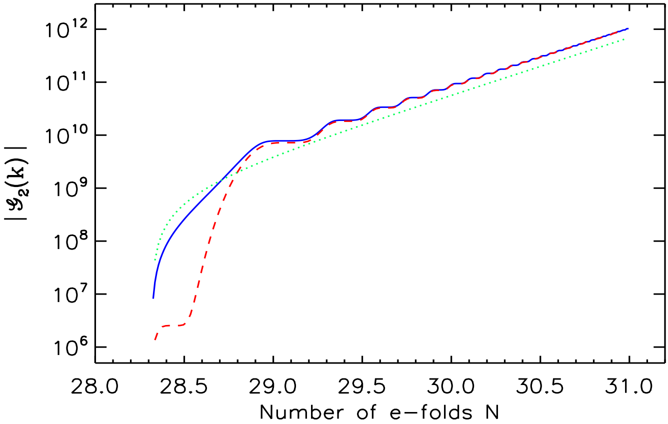

The behavior of the quantity $\mathcal{G}_2(\boldsymbol{k}_1, \boldsymbol{k}_2, \boldsymbol{k}_3)$ in the equilateral limit for a mode that leaves the Hubble radius at about 20 e-folds before the end of inflation. The blue curve represents the numerical result, while the dashed red curve denotes the analytical result[42].

[42] D. K. Hazra, J. Martin and L. Sriramkumar, Phys. Rev. D **86**, 063523 (2012).

An estimate of the contribution to $f_{\rm NL}^{\rm eq}$ during preheating

Upon assuming inflation to be of the power law form, the contribution to the non-Gaussianity parameter $f_{\rm NL}$ during preheating can be obtained to be

$$
\begin{aligned}
f_{\rm NL}^{\rm eq}(k) &= \frac{115\,\epsilon_1}{288\,\pi}\,\Gamma^2\left(\gamma+\frac{1}{2}\right)\,2^{2\,\gamma+1}\,(2\,\gamma+1)^2\,\sin\left(2\,\pi\,\gamma\right)\,\vert\gamma+1\vert^{-2\,(\gamma+1)}\\
&\times\left[1-{\rm e}^{-3\,(N_{\rm f}-N_{\rm e})/2}\right]\,\left[\left(\frac{\pi^2\,g_\ast}{30}\right)^{-1/4}\,(1+z_{\rm eq})^{1/4}\,\frac{\rho_{\rm cri}^{1/4}}{T_{\rm rh}}\right]^{-(2\,\gamma+1)}\\
&\times\left(\frac{k}{a_0\,H_0}\right)^{-(2\,\gamma+1)},
\end{aligned}
$$

where $g_\ast$ denotes the effective number of relativistic degrees of freedom at reheating, $T_{\rm rh}$ the reheating temperature and $z_{\rm eq}$ the redshift at the epoch of equality. Also, $\rho_{\rm cri}$, a_0 and H_0 represent the critical energy density, the scale factor and the Hubble parameter today, respectively.

For a model with $\gamma\simeq-2$ and a reheating temperature of $T_{\rm rh}\simeq 10^{10}$ GeV, one obtains that $f_{\rm NL}\approx 10^{-60}$ for the modes of cosmological interest (*i.e.* for k such that $k/a_0\simeq H_0$), a value which is completely unobservable[43].

[43] D. K. Hazra, J. Martin and L. Sriramkumar, Phys. Rev. D **86**, 063523 (2012).

Summary

- We have developed an efficient and robust procedure (and implemented it in BINGO) for numerically evaluating the scalar bispectrum in single field inflationary models.

Summary

- We have developed an efficient and robust procedure (and implemented it in BINGO) for numerically evaluating the scalar bispectrum in single field inflationary models.
- We find that the numerical results from BINGO match the spectral dependence in power law inflation as well as the analytical results available in the case of the Starobinsky model and slow roll inflation very well.

Summary

- We have developed an efficient and robust procedure (and implemented it in BINGO) for numerically evaluating the scalar bispectrum in single field inflationary models.
- We find that the numerical results from BINGO match the spectral dependence in power law inflation as well as the analytical results available in the case of the Starobinsky model and slow roll inflation very well.
- As an immediate application, we had investigated the power of the non-Gaussianity parameter $f_{_{\rm NL}}$ to be able to discriminate between different inflationary models that lead to deviations from slow roll and result in similar features in the scalar power spectrum. We find that certain differences in the background dynamics – reflected in the behavior of the slow roll parameters – can lead to a reasonably large difference in the $f_{_{\rm NL}}^{\rm eq}$ generated by the competing models.

Summary

- We have developed an efficient and robust procedure (and implemented it in BINGO) for numerically evaluating the scalar bispectrum in single field inflationary models.
- We find that the numerical results from BINGO match the spectral dependence in power law inflation as well as the analytical results available in the case of the Starobinsky model and slow roll inflation very well.
- As an immediate application, we had investigated the power of the non-Gaussianity parameter $f_{\rm NL}$ to be able to discriminate between different inflationary models that lead to deviations from slow roll and result in similar features in the scalar power spectrum. We find that certain differences in the background dynamics – reflected in the behavior of the slow roll parameters – can lead to a reasonably large difference in the $f_{\rm NL}^{\rm eq}$ generated by the competing models.
- Further, we have shown that, in single field inflationary potentials with a quadratic minimum, the contributions to the bispectrum during preheating proves to be completely negligible.

Thank you for your attention